

Absence of superconductivity and valence bond order in the Hubbard–Heisenberg model for organic charge-transfer solids

This article has been downloaded from IOPscience. Please scroll down to see the full text article.

2013 J. Phys.: Condens. Matter 25 385603

(<http://iopscience.iop.org/0953-8984/25/38/385603>)

View [the table of contents for this issue](#), or go to the [journal homepage](#) for more

Download details:

IP Address: 130.18.54.26

The article was downloaded on 13/09/2013 at 20:01

Please note that [terms and conditions apply](#).

Absence of superconductivity and valence bond order in the Hubbard–Heisenberg model for organic charge-transfer solids

N Gomes¹, R T Clay² and S Mazumdar¹

¹ Department of Physics, University of Arizona, Tucson, AZ 85721, USA

² Department of Physics and Astronomy and HPC² Center for Computational Sciences, Mississippi State University, Mississippi State, MS 39762, USA

E-mail: r.t.clay@msstate.edu

Received 11 June 2013, in final form 29 July 2013

Published 30 August 2013

Online at stacks.iop.org/JPhysCM/25/385603

Abstract

A frustrated, effective $\frac{1}{2}$ -filled band Hubbard–Heisenberg model has been proposed for describing the strongly dimerized charge-transfer solid families κ -(ET)₂X and Z[Pd(dmit)₂]₂. In addition to showing unconventional superconductivity, these materials also exhibit antiferromagnetism, candidate spin-liquid phases, and, in the case of Z = EtMe₃P, a spin-gapped phase that has sometimes been referred to as a valence bond solid. We show that neither superconductivity nor the valence bond order phase occurs within the Hubbard–Heisenberg model. We suggest that a description based on $\frac{1}{4}$ -filling, that is reached when the carrier concentration per molecule instead of per dimer is considered, thus may be appropriate.

(Some figures may appear in colour only in the online journal)

1. Introduction

Low-dimensional organic charge-transfer solids (CTS) are being intensively studied because of their many unusual competing and coexisting electronic phases. The most studied among them are probably the κ -(ET)₂X and Z[Pd(dmit)₂]₂ families, which, depending on the anion X[−] or cation Z⁺ exhibit unconventional superconductivity (SC), Néel antiferromagnetic (AFM) order, charge ordering (CO), candidate quantum spin-liquid (QSL) behavior, and supposedly also valence bond solid (VBS) order [1, 2]. The apparent similarity between these with the cuprate superconductors have been noted by many investigators. The semiconductor–SC transition in the CTS occurs under the application of pressure at constant carrier density, which suggests that the transition is driven by a small modification of a particular parameter of an appropriate Hamiltonian. The key questions then are, what is the minimal model, and which is the parameter whose changes give the competing phases.

Experimental observations appear to give a simple answer to these questions. The 2:1 (1:2) stoichiometry of κ -(ET)₂X (Z[Pd(dmit)₂]₂), indicates 0.5 hole (electron) per cationic (anionic) molecule. The crystal structures consist of

dimers of molecules arranged in an anisotropic triangular lattice. The strong role of repulsive electron–electron (e–e) Coulomb interactions is indicated by the observation of Néel AFM in κ -(ET)₂Cu[N(CN)₂]Cl and a candidate QSL phase in κ -(ET)₂Cu₂(CN)₃ [1]. A nonmagnetic state with spin gap has been found in EtMe₃P[Pd(dmit)₂]₂, and has been referred to as a VBS [2]. The VBS also requires strong e–e interactions, and furthermore, pressure-induced SC from this so-called VBS phase has been observed [3]. Considering the strongly correlated natures of the insulating states proximate to SC–AFM, QSL and VBS—the *effective* $\frac{1}{2}$ -filled band Hubbard model, or some variant of it, appears to be the appropriate minimal model, with the dimer units as the sites. The anisotropy of the triangular lattice, i.e., the degree of frustration, is the variable parameter that changes under external pressure or internal pressure effect caused by counter-ions with large size. Such a picture readily explains the observed commensurate AFM at large anisotropy. Motivated by Anderson’s resonating valence bond (RVB) theory [4] many investigators have proposed that the QSL and VBS phases can be explained within the correlated effective $\frac{1}{2}$ -filled band scenario. For moderate Hubbard U , an AFM semiconductor–paramagnetic metal (PM) transition

occurs with increasing frustration. D-wave SC mediated by fluctuations of the AFM ordering at the AFM–PM boundary has been also proposed based on mean-field and dynamic mean-field theories (DMFT) [5–12].

Numerical calculations have, however, failed to find SC within the triangular lattice $\frac{1}{2}$ -filled band Hubbard model [13–15]. Numerical studies have also failed to find a VBS phase in the model [16]. Although the $\frac{1}{2}$ -filled Hubbard model on the anisotropic triangular lattice does not appear to support SC, closely related models continue to be suggested as the appropriate theoretical model for describing the SC transition in the CTS. It has been claimed that the simple Hubbard model does not include all the spin–spin interactions that play an important role in the CTS, and that additional spin exchange unrelated to the Hubbard U must be incorporated to correctly capture AFM fluctuation effects [10–12, 17]. This has led to theoretical works on the so-called Hubbard–Heisenberg model given below. The goal of this paper is to critically examine whether the addition of a Heisenberg exchange term, assumed to be independent of the Hubbard onsite interaction U , causes a superconducting phase to occur in the $\frac{1}{2}$ -filled band anisotropic triangular lattice model. A second objective is to see whether the combined effects of U, J , and frustration can give the nonmagnetic insulating state found in $\text{EtMe}_3\text{P}[\text{Pd}(\text{dmit})_2]_2$ [2]. It is relevant in this context to point out that whether or not a VBS phase exists within the so-called J_1 – J_2 Heisenberg spin Hamiltonian, with spin exchange J_1 between nearest neighbors of a square lattice and J_2 along one diagonal bond, was controversial until recently [18, 19]. The similarity between the J_1 – J_2 spin Hamiltonian and the triangular lattice Hubbard–Heisenberg Hamiltonian (see below), taken together with the finite U in the latter, gives additional motivation for the current work.

2. Results

We consider the following Hamiltonian,

$$H = -t \sum_{\langle ij \rangle} B_{i,j} - t' \sum_{\{ij\}} B_{i,j} + U \sum_i n_{i\uparrow} n_{i\downarrow} + J \sum_{\langle ij \rangle} \vec{S}_i \cdot \vec{S}_j + J' \sum_{\{ij\}} \vec{S}_i \cdot \vec{S}_j. \quad (1)$$

In equation (1) sites $\langle ij \rangle$ are nearest neighbors on a square lattice while sites $\{ij\}$ are the next-nearest neighbors across a diagonal of each square plaquette. $B_{i,j} = \sum_{\sigma} (c_{i,\sigma}^{\dagger} c_{j,\sigma} + \text{H.c.})$, where $c_{i,\sigma}^{\dagger}$ creates an electron of spin σ on site i ; $n_{i\sigma} = c_{i\sigma}^{\dagger} c_{i\sigma}$. \vec{S}_i is the (spin- $\frac{1}{2}$) spin operator for site i . All energies will be given in units of t . We limit our analysis here to the region of lattice anisotropy appropriate for the title materials, $t' \lesssim 1$ [20–22].

We consider two limiting cases: (i) $J' = 0$, when the added Heisenberg interactions do not frustrate Néel antiferromagnetism, and (ii) $J' = J$, which frustrates the AFM state. The $J' = 0$ limit was studied by Gan *et al* using renormalized mean-field theory [10] and by Guertler *et al* using variational Monte Carlo [17] while the $J' = J$ limit was

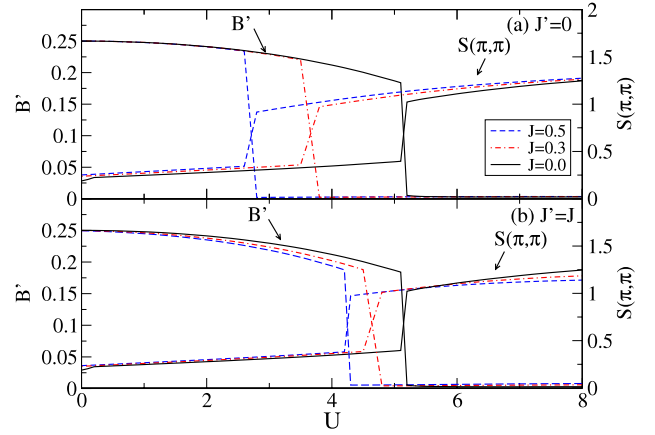


Figure 1. Diagonal bond order B' and spin structure factor $S(\pi, \pi)$ versus U for $t' = 0.4$. (a) $J' = 0$ (b) $J' = J$. Points are calculated at a spacing of $\Delta U = 0.1$. The J interaction strengthens the AFM phase.

investigated by Rau and Kee using a slave-rotor mean-field theory [12]. Powell and McKenzie studied variable J' [$0 < J'/J < 2$] using an RVB ansatz [11]. SC was found in some region of the parameter space by all of these authors. Several authors also found a spin-liquid phase [11, 12]. Rau and Kee examined the isotropic lattice and in addition found a VBS phase [12] that was claimed to explain the VBS-like order in $\text{EtMe}_3\text{P}[\text{Pd}(\text{dmit})_2]_2$ [2].

Here we examine the ground state of equation (1) using exact diagonalization of a 4×4 lattice. Exact diagonalization was previously used to study the model in the limit $J = 0$, concluding that no SC or enhancement of the pairing correlations by U is present [13]. Despite the small-lattice size (even smaller lattices are however used in cluster DMFT calculations [9]) the validity of these 4×4 results has been confirmed by recent path integral renormalization group (PIRG) [23] calculations on considerably larger lattices [14] that arrived at even stronger conclusions regarding the absence of SC.

It will be useful to briefly recall the ground state phase diagram in the $J = J' = 0$ limit [13–16, 24–28]. Known ground state phases include two AFM phases with Néel and 120° order, a PM phase and a gapless nonmagnetic insulator (NMI) or QSL phase [13, 14, 16, 24–28]. The NMI phase is found between the AFM and PM phases for $t' \gtrsim 0.5$ [24, 25]. Near the isotropic lattice ($t' \approx t$) magnetically ordered states with $\mathbf{Q} \neq (\pi, \pi)$ are found for large U [13, 26, 28]. However, such non-Néel AFM ordering is not found experimentally [1].

We first consider the $t' \lesssim 0.5$ region of the phase diagram where a direct PM–AFM transition is found for $J = J' = 0$. We have calculated the diagonal bond order $B' \equiv \langle B_{i,j} \rangle$ for sites i and j connected by the t' bond and the spin structure factor

$$S(\mathbf{Q}) = \frac{1}{N} \sum_{j,k} e^{i\mathbf{Q} \cdot (\mathbf{r}_j - \mathbf{r}_k)} \langle (n_{j,\uparrow} - n_{j,\downarrow})(n_{k,\uparrow} - n_{k,\downarrow}) \rangle. \quad (2)$$

Figures 1(a) and (b) show B' and $S(\pi, \pi)$ versus U for $t' = 0.4$ and several different J (0, 0.3, 0.5). A sudden drop in B' at $U = U_c$, simultaneous with a sudden increase in $S(\pi, \pi)$,

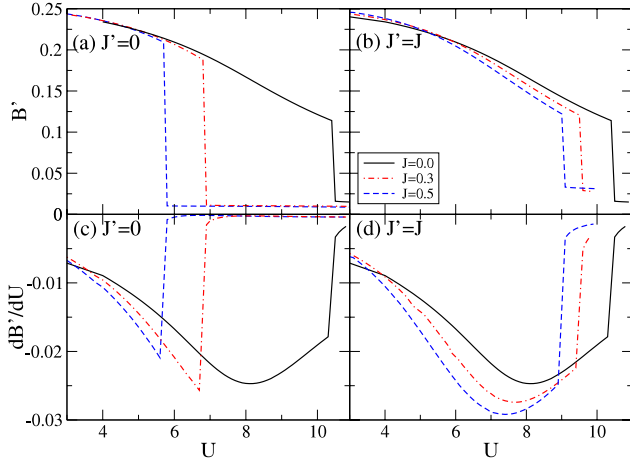


Figure 2. Diagonal bond order B' versus U for $t' = 0.8$ with (a) $J' = 0$, and (b) $J' = J$. The derivative of B' , dB'/dU with (c) $J' = 0$ and (d) $J' = J$. B' is calculated for points separated by $\Delta U = 0.1$. For $J' = 0$ no NMI phase is found. When $J' \neq 0$, both PM–NMI and NMI–AFM phase boundaries shift to smaller U . The solid, dashed–dotted and dashed curves correspond to $J = 0.0, 0.3$, and 0.5 , respectively.

indicates transition to an insulating AFM state [13, 25]. For both $J' = 0$ and $J' = J$, J lowers the U_c for transition to AFM, broadening the AFM region. As shown in figure 1 the largest broadening occurs when $J' = 0$.

As t' increases the size of the discontinuity in B' and $S(\pi, \pi)$ decreases. This is due to the appearance of a NMI phase in between the PM and AFM phases for $t' \gtrsim 0.5$ [24, 25]. While the transition between PM and AFM phases for $t' \lesssim 0.5$ is discontinuous as U is varied, for larger t' the PM–NMI transition at U_{c1} and the NMI–AFM transition at U_{c2} are continuous [25]. The continuous PM–NMI and NMI–AFM transitions cannot be captured from calculations of B' , $\langle n_{\uparrow} n_{\downarrow} \rangle$ or $S_{\sigma}(\pi, \pi)$. As noted previously [13] for $J = J' = 0$, derivatives dB'/dU or $d\langle n_{\uparrow} n_{\downarrow} \rangle/dU$ can be used to determine U_{c1} and U_{c2} . Critical values obtained by the two methods differ by 0.1 at most. In the present case, J and J' have nearly negligible effects on $\langle n_{\uparrow} n_{\downarrow} \rangle$, which is why we have determined U_{c1} and U_{c2} from calculations of dB'/dU . In figure 2 we plot B' versus U and its derivative dB'/dU for $t' = 0.8$, calculated using a centered-difference approximation with a U grid of $\Delta U = 0.1$. We find that for $J' = 0$ (figures 2(a) and (c)), the stability of the AFM phase is enhanced by U ; U_{c1} decreases with J . At the same time, the NMI phase is suppressed: the inflection point in B' in figure 2(a) for $J = 0$ and the corresponding minimum in dB'/dU in figure 2(c) disappear even for quite small values of J . For $J' = J$ (figures 2(b) and (d)), the system progresses through two transitions, PM–NMI and NMI–AFM, as in the pure Hubbard model. As seen in figures 2(b) and (d), there is a slight narrowing of the NMI phase.

A necessary condition for SC is that the pair–pair correlation function $P(r)$ for pairs of appropriate symmetry reaches a constant value as $r \rightarrow \infty$. An additional requirement for SC mediated by interactions is that the pair–pair correlations are enhanced by the interaction [13]. In exact

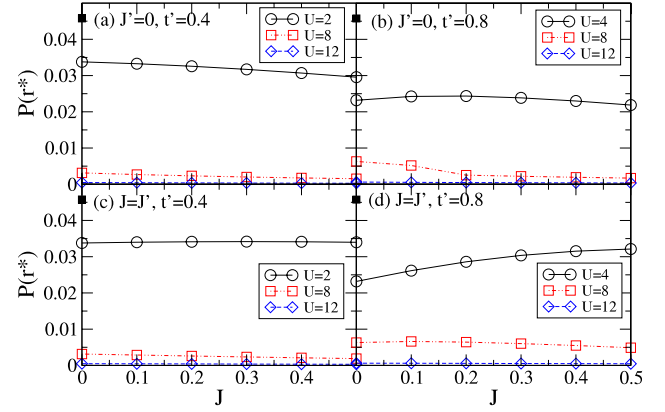


Figure 3. Long-range $d_{x^2-y^2}$ pair–pair correlation function $P(r^*)$ (see text) as a function of J for (a) $t' = 0.4$, $J' = 0$, (b) $t' = 0.8$, $J' = 0$, (c) $t' = 0.4$, $J' = J$, and (d) $t' = 0.8$, $J' = J$. $P(r^*)$ at $U = J = 0$ is shown by the filled square on each plot. Independent of the value of J , long-range pair–pair correlations decrease monotonically as U increases.

diagonalization studies of the $J = 0$ model, $P(r)$ for all symmetries was found to decrease monotonically with U from the $U = 0$ limit [13]. Large-lattice studies found further that *as a function of distance r* , the magnitude of $P(r)$ decreased with distance faster than the $U = 0$ solution [14]. These two results indicated that SC is not present in the $J = 0$ limit. Here we focus on any possible enhancement of $P(r)$ due to J .

We calculate the pair–pair correlation function as a function of distance, $P(r) = \langle \Delta_i^\dagger \Delta_{i+\vec{r}} \rangle$, where pair-creation operators Δ_i^\dagger are defined as

$$\Delta_i^\dagger = \frac{1}{\sqrt{2}} \sum_{\vec{v}} g(\vec{v}) (c_{i,\uparrow}^\dagger c_{i+\vec{v},\downarrow}^\dagger - c_{i,\downarrow}^\dagger c_{i+\vec{v},\uparrow}^\dagger). \quad (3)$$

The phases $g(\vec{v})$ determine the symmetry of the superconducting pairs. In our calculations we considered s, $d_{x^2-y^2}$, and d_{xy} pairing symmetries [13]. Out of these pairing symmetries, we found that for $t' < t$, $P(r)$ is largest for $d_{x^2-y^2}$ pairing symmetry.

Although we have calculated $P(r)$ for all r we show here our results for the largest possible r , r^* . Figure 3 shows the pair–pair correlation $P(r^*)$ as a function of J for $d_{x^2-y^2}$ pair symmetry. Representative values of U are chosen in each panel to correspond to the different regions of the phase diagram (PM, AFM, NMI). In figures 3(a) and (b) we take $J' = 0$ and two different values of t' , 0.4 and 0.8. In both figures 3(a) and (b) a direct PM–AFM transition exists. As with $J = 0$ [13], $P(r^*)$ decreases monotonically with U , with its value decreasing discontinuously at the PM–AFM transition. As figures 3(a) and (b) show, $P(r^*)$ also decreases monotonically with J for $J' = 0$. The primary effect of J here is to expand the AFM region (figure 1), which *decreases* the potential phase space available for SC. In figures 3(c)–(d) we take $J' = J$. In figure 3(c), $t' = 0.4$ and again there are only PM and AFM phases. The behavior is very similar to the $J' = 0$ case. Figure 3(d) is for $J' = J$ and $t' = 0.8$, with U values chosen to represent points in the PM, NMI, and AFM phases. In the PM region for large t' ($t' \gtrsim 0.7$) there is a small increase

of $P(r^*)$ with J , but $P(r^*)$ remains considerably below its uncorrelated value. Pairing correlations continue to decrease monotonically with U .

Summarizing our results for the $d_{x^2-y^2}$ pair-pair correlations, for $t' \lesssim 0.7$, J and J' decrease $P(r)$. In the larger t' region, although there is a weak enhancement of $P(r)$ compared to $J = J' = 0$, the pair correlations never exceed the value obtained for the uncorrelated limit.

In view of the absence of SC found in our calculations, it is of some interest to determine how these results, primarily for the strong coupling regime, extrapolate to earlier weak coupling (small $U/|t|$) calculations on the Hubbard model based on the renormalization group approach [29]. These latter calculations do find robust SC within the model, although the predicted critical temperatures are very small. A direct comparison of our work with the weak coupling approach is difficult for several reasons. First, lattices far larger than the present 4×4 would be required to resolve the non-local pairing functions appropriate for the weak coupling model. Secondly, the competition with AFM, ignored within the weak coupling calculation, is relevant within the half-filled model even for small U . We have, for example, found discernible AFM with peak in $S(\pi, \pi)$ for $U/|t|$ as small as 0.5 and small t' . This interaction strength is already much smaller than estimates of U/t for the κ -(ET)₂X and Z[Pd(dmit)₂]₂ materials.

The compound EtMe₃P[Pd(dmit)₂]₂ exhibits a spin gap below 25 K [2]. The low temperature phase has been described as a VBS by the original investigators [2]. Pressure-induced VBS–SC transition, –analogous to the AFM–SC and QSL–SC transitions in the κ -(ET)₂X –occurs in EtMe₃P[Pd(dmit)₂]₂. Any candidate model that is valid for CTS with dimerized units should therefore have VBS order in some region of the phase diagram. Further motivation to find VBS phases in models of interacting electrons comes from the extensive recent theoretical investigations of frustration-driven AFM–VBS quantum phase transitions within quantum spin models [18, 19]. The VBS phase, if it at all appears within the present model, should appear in the highly frustrated region of the phase diagram. This is in agreement with the estimation of $t'/t \approx 0.9$ in EtMe₃P[Pd(dmit)₂]₂, obtained from *ab initio* calculation [22]. In the context of the present model the parameter region of interest is large U with $t' \sim t$, in between the Néel and 120° AFM phases. Previous PIRG numerical studies [16] as well as more recent work [30] on the Hubbard ($J' = J = 0$) model have, however, found the NMI rather than VBS in this region.

As with SC, the VBS phase has been claimed within slave-rotor theory for the isotropic Hubbard–Heisenberg model ($t' = t$, $J' = J$) for both $J = 0$ and $J > 0$ [12]. The J interaction was found to strengthen the VBS order [12]. We therefore investigate the Hubbard–Heisenberg Hamiltonian in this highly frustrated region. The VBS order parameter is the bond–bond structure factor $S_B^x(\mathbf{Q})$ for bonds along the x axis, defined as

$$S_B^x(\mathbf{Q}) = \frac{1}{N} \sum_{i,j} e^{i\mathbf{Q}\cdot\mathbf{r}_{ij}} \langle (B_{i,i+\hat{x}} - \langle B \rangle)(B_{j,j+\hat{x}} - \langle B \rangle) \rangle, \quad (4)$$

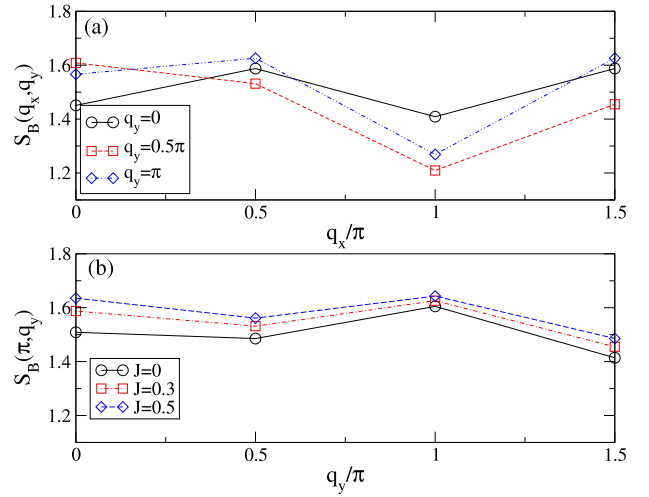


Figure 4. (a) Bond–bond structure factor $S_B^x(q_x, q_y)$ as a function of q_x, q_y for $t' = 0.9$, $U = 8$, and $J' = J = 0.3$. (b) $S_B^x(\pi, q_y)$ for $U = 8$ and varying J . Lines are only guides to the eye.

where $\langle B \rangle$ is the expectation value of the bond order. We consider just the $J' = J$ case, as no NMI phase exists when $J' = 0$ (see figure 2). VBS order with columnar dimer pattern as claimed in [12] would correspond to a peak in $S_B^x(\mathbf{Q})$ at $\mathbf{Q} = (\pi, 0)$. Figure 4(a) shows $S_B^x(\mathbf{Q})$ for $U = 8$, $t' = 0.9$, and $J' = J = 0.3$. Throughout the NMI region ($6 \lesssim U \lesssim 12$) we find no changes in the \mathbf{Q} -dependence of $S_B^x(\mathbf{Q})$. As shown in figure 4(a), all orderings with $q_x = \pi$, corresponding to bond alternation along x , are *suppressed* compared to other values of q_x . Figure 4(b) shows the J dependence of $S_B^x(q_x = \pi, q_y)$. As J increases, no peaks develop; rather the effect of J is simply a renormalization affecting all $S_B^x(\mathbf{Q})$ at all \mathbf{Q} equally. Since the VBS order is absent within the NMI phase for $J = 0$ to begin with [16], this is strong evidence that the J interaction does not lead to a VBS phase. Our result is in agreement with that obtained in [18, 19], who noted the absence of the VBS within the J_1 – J_2 model, which is the $U \rightarrow \infty$ limit of our Hamiltonian equation (1).

3. Discussion

In summary, the inclusion of Heisenberg exchange interactions in the effective $\frac{1}{2}$ -filled band for κ -(ET)₂X and Z[Pd(dmit)₂]₂ merely strengthens the AFM phase, and either eliminates the NMI phase (for $J' = 0$) or reduces its width in the phase diagram (for $J' \neq 0$). Importantly, neither SC nor VBS phases are present in the $\frac{1}{2}$ -filled band model for any realistic J . The phase diagram (figure 5) remains nearly identical with the phase diagram of the bare $\frac{1}{2}$ -filled Hubbard model [13, 14]. The absence of SC and VBS phases in our phase diagram indicates that while the approximate methods used previously can correctly predict AFM, which is a classical ordering, they predict spurious spin-singlets, the formation of which is a quantum mechanical effect.

The question that we started with—what is the minimal model that describes the complete phase diagram of the CTS—then continues to be relevant. Our current finite

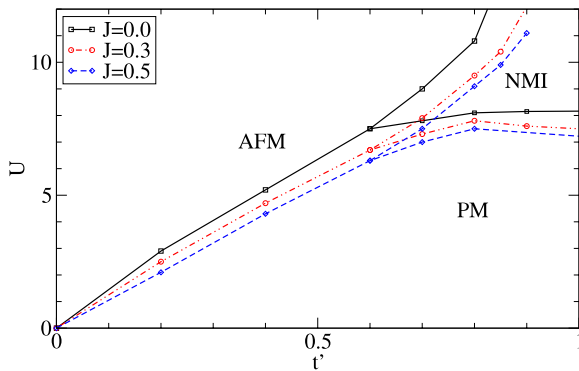


Figure 5. The phase diagram with $J' = J$ for parameter regions relevant for the dimerized CTS.

size calculations suggest that purely electronic $\frac{1}{2}$ -filled band models in which short-range e–e and spin–spin interactions, together with lattice frustration, are the driver of SC may not be the appropriate choices. As in the case of $J = 0$, we intend to extend our calculations to larger lattices using the PIRG technique in the future. In principle this still leaves open the possibility that there exist other variants of the $\frac{1}{2}$ -filled band correlated-electron model, with or without electron–phonon interactions, that may be suitable. To the best of our knowledge no such theoretical scenario has been proposed yet. In the absence of such work in the existing literature we suggest that the interacting frustrated $\frac{1}{4}$ -filled band model proposed by us [31, 32] and others [33, 34] is a likely choice for the correct theoretical model. Within this latter model, the number of charge carriers *per molecule*, rather than per dimer unit cell is the relevant parameter. This proposal has several apparent advantages over effective $\frac{1}{2}$ -filled band models. First, it applies equally well to both the dimerized κ -(ET)₂X and Z[Pd(dmit)₂]₂ and the undimerized θ -(ET)₂X which show CO–SC (as opposed to AFM–SC) transitions. As also pointed out in [35], there exist many other exotic superconductors which coincidentally or otherwise share this same bandfilling. Second, we have recently shown that a frustration-driven AFM–spin singlet transition occurs within the dimerized interacting $\frac{1}{4}$ -filled band model, where the spin singlet state coexists with CO [32, 36]. Structural analysis shows that the so-called VBS state in EtMe₃[Pd(dmit)₂]₂ has the same CO pattern [2, 37] as that in the coexisting CO–spin singlet found by us in the frustrated $\frac{1}{4}$ -filled band [32, 36]. Finally, experiments have found evidence for charge fluctuations in the QSL state of κ -(ET)₂Cu₂(CN)₃ [38], which is clearly not possible within the $\frac{1}{2}$ -filled band scenario. The work reported here then gives added motivation to search for frustration-induced SC within the correlated $\frac{1}{4}$ -filled band model. Work is currently in progress in this direction.

Acknowledgments

Work by NG was supported by NSF-CHE-1151475. Work by RTC and SM was supported by the Department of Energy grant DE-FG02-06ER46315.

References

- [1] Kanoda K and Kato R 2011 *Annu. Rev. Condens. Matter Phys.* **2** 167
- [2] Tamura M and Kato R 2009 *Sci. Technol. Adv. Mater.* **10** 024304
- [3] Shimizu Y, Akimoto H, Tsujii H, Tajima A and Kato R 2007 *Phys. Rev. Lett.* **99** 256403
- [4] Anderson P W 1973 *Mater. Res. Bull.* **8** 153–60
- [5] Schmalian J 1998 *Phys. Rev. Lett.* **81** 4232–5
- [6] Kino H and Kontani H 1998 *J. Phys. Soc. Japan* **67** 3691
- [7] Kondo H and Moriya T 1998 *J. Phys. Soc. Japan* **67** 3695
- [8] Vojta M and Dagotto E 1999 *Phys. Rev. B* **59** R713–6
- [9] Kyung B and Tremblay A M S 2006 *Phys. Rev. Lett.* **97** 046402
- [10] Gan J Y, Chen Y, Su Z B and Zhang F C 2005 *Phys. Rev. Lett.* **94** 067005
- [11] Powell B J and McKenzie R H 2005 *Phys. Rev. Lett.* **94** 047004
- [12] Powell B J and McKenzie R H 2007 *Phys. Rev. Lett.* **98** 027005
- [13] Rau J G and Kee H-Y 2011 *Phys. Rev. Lett.* **106** 056405
- [14] Clay R T, Li H and Mazumdar S 2008 *Phys. Rev. Lett.* **101** 166403
- [15] Dayal S, Clay R T and Mazumdar S 2012 *Phys. Rev. B* **85** 165141
- [16] Tocchio L F, Parola A, Gros C and Becca F 2009 *Phys. Rev. B* **80** 064419
- [17] Watanabe S 2003 *J. Phys. Soc. Japan* **72** 2042–5
- [18] Guertler S, Wang Q H and Zhang F C 2009 *Phys. Rev. B* **79** 144526
- [19] Jiang H-C, Yao H and Balents L 2012 *Phys. Rev. B* **86** 024424
- [20] Hu W J, Becca F, Parola A and Sorella S 2013 arXiv:1304.2630
- [21] Kandpal H C, Opahle I, Zhang Y-Z, Jeschke H O and Valentí R 2009 *Phys. Rev. Lett.* **103** 067004
- [22] Nakamura K, Yoshimoto Y, Kosugi T, Arita R and Imada M 2009 *J. Phys. Soc. Japan* **78** 083710
- [23] Scriven E P and Powell B J 2012 *Phys. Rev. Lett.* **109** 097206
- [24] Kashima T and Imada M 2001 *J. Phys. Soc. Japan* **70** 2287–99
- [25] Kashima T and Imada M 2001 *J. Phys. Soc. Japan* **70** 3052
- [26] Morita H, Watanabe S and Imada M 2002 *J. Phys. Soc. Japan* **71** 2109–12
- [27] Mizusaki T and Imada M 2006 *Phys. Rev. B* **74** 014421
- [28] Koretsune T, Motome Y and Furusaki A 2007 *J. Phys. Soc. Japan* **76** 074719
- [29] Yoshioka T, Koga A and Kawakami N 2009 *Phys. Rev. Lett.* **103** 036401
- [30] Raghu S, Kivelson S A and Scalapino D J 2010 *Phys. Rev. B* **81** 224505
- [31] Tocchio L F, Feldner H, Becca F, Valentí R and Gros C 2013 *Phys. Rev. B* **87** 035143
- [32] Mazumdar S and Clay R T 2008 *Phys. Rev. B* **77** 180515(R)
- [33] Li H, Clay R T and Mazumdar S 2010 *J. Phys.: Condens. Matter* **22** 272201
- [34] Naka M and Ishihara S 2010 *J. Phys. Soc. Japan* **79** 063707
- [35] Hotta C 2010 *Phys. Rev. B* **82** 241102
- [36] Mazumdar S and Clay R T 2012 *Phys. Status Solidi b* **249** 995
- [37] Dayal S, Clay R T, Li H and Mazumdar S 2011 *Phys. Rev. B* **83** 245106
- [38] Yamamoto T, Nakazawa Y, Tamura M, Nakao A, Ikemoto Y, Moriwaki T, Fukaya A, Kato R and Yakushi K 2011 *J. Phys. Soc. Japan* **80** 123709
- [39] Abdel-Jawad M, Terasaki I, Sasaki T, Yoneyama N, Kobayashi N, Uesu Y and Hotta C 2010 *Phys. Rev. B* **82** 125119